

Point Spread Functions of defocused Leaky Annular Apertures with Spherical Aberration

N. Sabitha^{1*} and D. Karuna Sagar¹

¹Optics Research Group, Department of Physics, Osmania University, Hyderabad-500007, India

Abstract:

The point spread function of the optical system in the presence of defocus and primary spherical aberration with the complex Hanning filter with amplitude and phase has been investigated. A substantial improvement in the intensity profile of the impulse response of the optical system has been achieved. When the optical system is subjected to higher orders of aberration and apodization, the optical system behaves like a super-resolver with lateral resolution of the central peak being improved radically. The presence of first minima with zero intensity suits the optical system to be applied for two-point resolution studies in terms of Rayleigh criterion.

Keywords: Amplitude Apodization, Defect-of-focus, Hanning filter, Point Spread Function, Primary Spherical Aberration.

Date of Submission: 14-03-2023

Date of Acceptance: 30-03-2023

I. Introduction

The point spread function (PSF) describes the response of an imaging system to a point source or a point object. A more general term for the PSF is a system's impulse response, the PSF being the impulse response of focused optical system. The PSF in many contexts can be thought of as the extended blob in an image that represents a single point object. In functional terms, it is the spatial domain version of the optical transfer function of the imaging system[1]. PSF engineering is the modulation of the light distribution in the focal region of the optical system, exploited for improving the performance of an optical system employed in numerous applications. This mechanism when demonstrated by inserting suitable phase or amplitude filters in the Fourier plane of the optical system, results in the changes in the intensity level of the central maxima and its surrounding side lobes[2].

Apodization can be achieved in a number of methods, including changing the geometry of aperture or transmission qualities [1]. The former is referred to as aperture shaping and it involves changing the shape and size of the aperture. Secondly an apodized filter over the pupil known as aperture shading. Thus, apodization is the deliberate manipulation of the pupil function to change the light distribution in the PSF in order to improve the quality of image [2]. In optics, apodization is comparable to pulse shaping in electrical engineering [3, 4]. Straubel is credited as being the inventor of apodization theory [5]. The higher spatial frequencies are reduced as the amplitude transmittance of the pupil is gradually reduced from the centre to the edge of the pupil, resulting in suppression of side lobes. Apodization is a subset of the more general spatial filtering approach (Hecht and Zajac, 1987). Apodization can help an aberrated optical system improve certain aspects of its imaging performance [6-8]. With the goal of improving image quality, some researchers have investigated the edge-ringing and edge-shifting aspects of various pupil functions [9-11]. The difference between the first maximum of the edge fringes and the unit object intensity is the edge ringing. Edge-shift, also known as image shift, is the distance between the image edge and half of the object edge's intensity value. The rise in image intensity over a unit change in Z around the geometric edge (i.e., Z=0) is known as an edge-gradient. To avoid edge-ringing in coherent and partially coherent illuminations, it is desirable to build a system that produces actual and positive amplitude impulse. This problem has been investigated, and it has been determined that proper apodizer can control edge-ringing [12-14]. In the absence and presence of aberrations, aperture shaping reduces the negative effects of edge-ringing in coherent image. The appearance of a sharp cut-off in the transfer function distinguishes a coherent optical system. The high frequency components of an edge object are quite powerful. When compared to the Fourier spectrum of the sharp edge, the coherent optical system's cut-off is effectively low, resulting in undesirable edge ringing [15].

Apodization can be employed for a variety of objectives, including suppressing optical side-lobes in an optical imaging system's diffraction field [16-17], enhancing depth of field [18-22], and improving resolution [23-28]. The effectiveness of the apodization technique is constantly linked to the design of pupil function. It is well known that apodization, which is used to lower the size of the point spread function's focus spot, frequently

results in the growth of side lobes. As a result, many techniques to reaching a compromise are examined [29-33].

Theory and Formulation

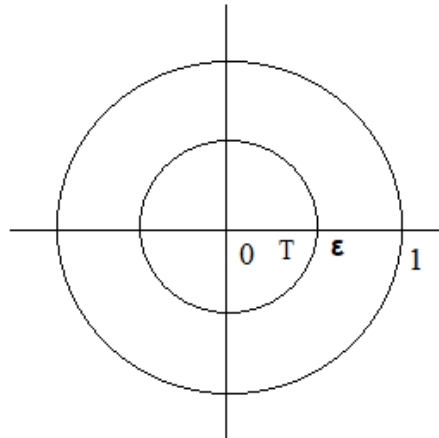


Figure.1 Leaky Annular Aperture

Figure 1 shows the leaky annular aperture with transmission factor ‘T’ and ‘ε’ is the partition parameter for the central zone. Phase filter is introduced for the central zone, i.e., from 0 to ε and Hanning amplitude filter is applied for the outer zone, i.e., from ε to 1.

The present study is projected to evaluate the effect of the Hanning amplitude filter with phase on the optical system which is under the combined influence of high primary spherical aberration and defect-of-focus.

The far-field diffraction characteristics due to a circular aperture in an optical imaging system can be derived from its amplitude response or amplitude PSF. The diffracted light amplitude associated with a rotationally symmetric pupil is given by

$$A(Z) = 2 \int_0^1 f(r) J_0(Zr) r dr \tag{1}$$

Here ‘ J_0 ’ is the Bessel function of the first kind and zero order and ‘r’ is the normalised distance from a point on the exit pupil of the system is varying from 0 to 1, also known as the radial coordinate in the pupil plane. ‘Z’ is the reduced dimensionless diffraction coordinate in the image plane.

The expression for the leaky annular aperture for the chosen amplitude filter is given by

$$A(Z) = 2 \left[\int_0^\epsilon T e^{-i\pi} J_0(Zr) r dr + \int_\epsilon^1 f(r) e^{-i(\phi_a + \phi_s)} J_0(Zr) r dr \right] \tag{2}$$

Where ϕ_a and ϕ_s are the defect-of-focus and primary spherical aberration parameters, T is the transmission factor in the leaky zone and ε is the partition parameter for the central zone of the circular aperture.

In the present study, we have considered the Hanning amplitude filter whose pupil function can be represented by

$$f(r) = \cos(\pi\beta r) \tag{3}$$

We have considered the variable apodization with two zones of the circular aperture with central zone being leaky by the transmission factor ‘T’ while the Hanning amplitude filter is controlling the transmission profile in the outer zone.

Where β is the apodising parameter controlling the non-uniform transmission of the pupil. The intensity PSF B(z) which is the real measurable quantity can be obtained from the squared modulus of A(z). Thus,

$$B(Z) = |A(Z)|^2 \tag{4}$$

II. Results and Discussions

The investigations on the effects of leaky aperture on the images of point objects formed by coherent optical systems apodized by the complex Hanning amplitude filter in the presence of defect-of-focus and primary spherical aberrations have been evaluated using the expression (4) by employing Matlab simulation. The intensity distribution B (Z) in the images of point objects has been obtained for different values of dimensionless diffraction variable Z varying from – 12 to + 12. The image quality assessment parameters such as

full-width at half-maximum(FWHM) and first maxima and first minima have been studied for various values of apodization, aberrations and leaky aperture transmission parameter.

In general, the intensity level of the first-order sidelobes and the FWHM of the central peak in the resulting intensity distribution are used to calculate the effect of pupil apodization. Therefore, in a variety of circumstances, the suggested apodization across the pupil reduces the light energy related to the first and higher order sidelobe levels of the PSF. According to the Rayleigh criterion [23], the transverse resolution of PSF grows as the FWHM of its central peak shrinks. In the presence of high aberrations, apodization ($\beta = 1$) across the pupil to reduce the higher frequency components at the edges of the pupil function, which lowers the FWHM of the central peak to a lower value. Here, the pupil transmission profile strongly depends on the value of β , as well as the amount and nature of aberrations considered in the optical system.

Figure 2 gives the pupil transmittance curves of the Hanning pupil. It illustrates the response of the amplitude transmittance $f(r)$ with the normalized distance ' r '. At the centre of the pupil i.e., $r = 0$, $f(r)$ is unity i.e., maximum for all values of apodization parameter β and it decreases towards the edges as r goes from 0 to 0.50. The amplitude transmittance ceases for $r = 0.5$, when $\beta=1$, for $r = 1$ when $\beta = 0.5$ respectively.

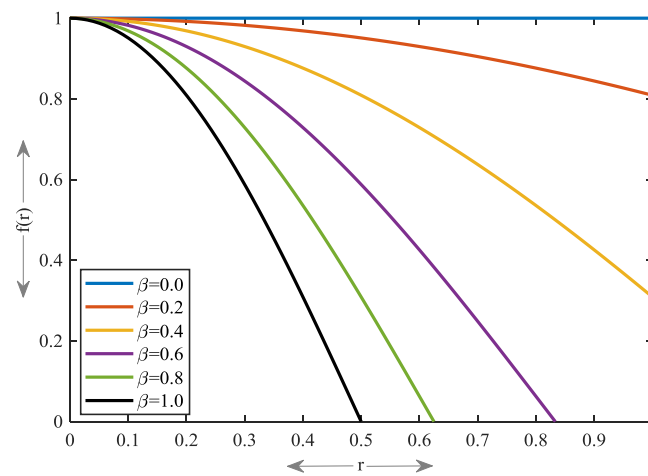


Figure 2: Pupil Transmission Profile of Hanning amplitude filter

Figure 3(a-e) depicts the effect of the apodization parameter β on the intensity distribution of PSF under various situations. With increase in the apodization, there is a decrease in the intensity of the central lobe. As the apodization parameter β is increased from $\beta=0$ to $\beta=0.6$, the optical side lobes are completely suppressed. However, for higher orders of apodization ($\beta=1$), the radius of the first dark ring in the diffraction pattern becomes less than that of Airy case.

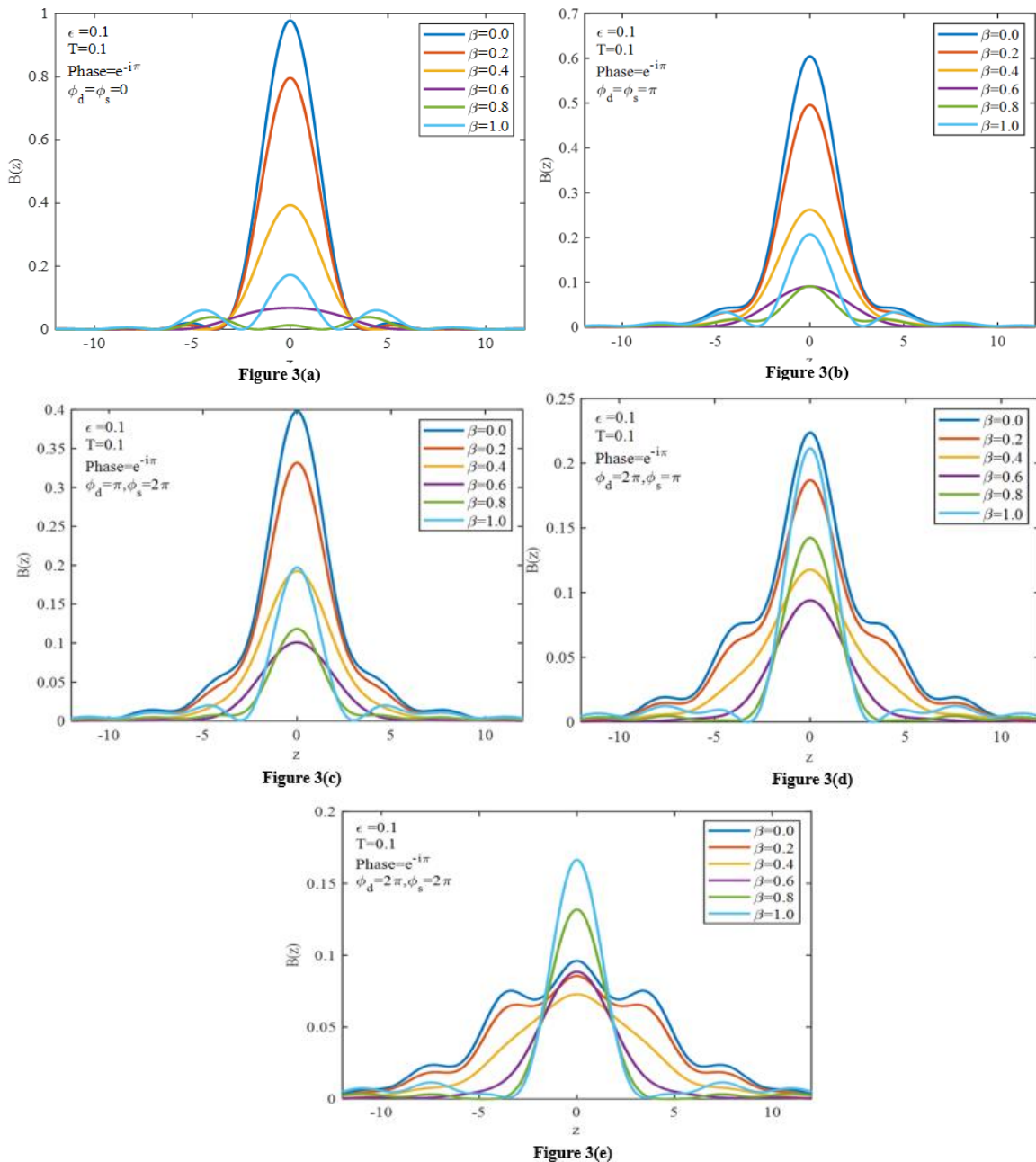


Figure 3(a-e) Intensity distribution curves for leaky aperture with apodization in the absence and presence of various degrees of defocus and spherical aberration

Table.1 Maxima Minima values

Phase= $e^{-i\pi}$	β	C.Max		F.Min		F.Max	
		Position	Value	Position	Value	Position	Value
Figure 3(a) $\epsilon=0.1, T=0.1$ $\phi_d=\phi_s=0$	0	0	0.9781	3.7813	0	5.1345	0.0204
	0.2	0	0.7965	3.8862	0	5.2206	0.0139
	0.4	0	0.3938	4.3923	0	5.6814	0.0032
	0.6	0	0.0683	5.9655	0	7.619	0.0016
	0.8	0	0.0134	1.6358	0	3.9809	0.0391
	1	0	0.1731	2.5014	0	4.4142	0.0611
Figure 3(b)	0	0	0.9781	3.7813	0	5.1345	0.0204
	0.2	0	0.7965	3.8862	0	5.2206	0.0139
	0.4	0	0.3938	4.3923	0	5.6814	0.0032
	0.6	0	0.0683	5.9655	0	7.619	0.0016
	0.8	0	0.0134	1.6358	0	3.9809	0.0391
	1	0	0.1731	2.5014	0	4.4142	0.0611

Point Spread Functions of defocused Leaky Annular Apertures with Spherical Aberration

	0	0	0.6045	6.929	0.0073	7.9688	0.0094
	0.2	0	0.4959	7.0128	0.0057	7.9658	0.0068
$\varepsilon=0.1, T=0.1$	0.4	0	0.262	10.7228	0
$\phi_d=\phi_s=\pi$	0.6	0	0.0909	5.8495	0.0011	7.1088	0.0015
	0.8	0	0.0913	2.9343	0.0131	4.0624	0.0169
	1	0	0.2073	2.8289	0.0022	4.5414	0.0332
<hr/>							
	0	0	0.3983	6.7397	0.0126	7.687	0.0143
	0.2	0	0.3317	6.821	0.0099	7.6648	0.0108
$\varepsilon=0.1, T=0.1$	0.4	0	0.1926
$\phi_d=\pi, \phi_s=2\pi$	0.6	0	0.1009	8.8856	0.0006	10.3029	0.0008
	0.8	0	0.1183	3.5462	0.0071	4.2107	0.0076
	1	0	0.1975	3.0112	0.0009	4.6692	0.02
<hr/>							
	0	0	0.2238	6.7273	0.0178	7.5879	0.0192
	0.2	0	0.1869	6.8452	0.0143	7.5451	0.0148
$\varepsilon=0.1, T=0.1$	0.4	0	0.1177
$\phi_d=2\pi, \phi_s=\pi$	0.6	0	0.0939	8.6398	0.0007	10.2787	0.0011
	0.8	0	0.1424	3.9885	0.0011	4.648	0.0013
	1	0	0.2116	3.2614	0	4.7627	0.0096
<hr/>							
	0	0	0.0962	2.1508	0.0692	3.3748	0.0753
	0.2	0	0.0857	2.3465	0.0647	3.0904	0.0656
$\varepsilon=0.1, T=0.1$	0.4	0	0.0729
$\phi_d=2\pi, \phi_s=2\pi$	0.6	0	0.0885	8.2537	0.0007	10.0378	0.0011
	0.8	0	0.1319	4.8428	0	7.3998	0.0034
	1	0	0.1665	3.5331	0.0011	7.4489	0.0116

Figure 3(e) represents the intensity distribution profiles for higher values of defect-of-focus and primary spherical aberration, i.e., for $\phi_d=2\pi$ and $\phi_s=2\pi$. For $\beta=0.8$ and $\beta=1$, the first minima and the side-lobes on both sides of the main peak reaches to zero and the intensity of the main peak is considerably improved. The point spread function modifies into a super-resolved point spread function with increase in the intensity above that of the Airy case with reduction in the width of the central lobe. It is observed that for $\beta=0$ (Airy case), in the presence of high degree of spherical aberration and defocus intensity of the principal maximum is highly distorted. Here the intensity of the secondary maxima is high and its axial shape or resolution is found to be poor with non-zero first minima. In the presence of defocusing effect and aberration, as the degree of apodization increases from 0.4 to 1 (as shown in figure.2), there exists a consistent improvement in the lateral resolution of the main peak. It is clearly observed that for highest degree of apodization ($\beta=1$), the central light flux exhibit high intensity compared to that of Airy case ($\beta=0$) and along with zero intensity in the first minima is measured as radius of the first dark ring, resulting in super-resolved point spread function. Figure 3(e) represents the highly aberrated PSF, for $\beta=0.8$ and $\beta=1.0$, the first minima intensity is zero. And the central peak has high intensity compared to that of Airy case $\beta=0$. This is one of the desirable features in the super-resolved point spread function.

It is also observed that, from Table 1, for higher values of β with induced phase π , first minima intensity value almost reaches zero, for $\beta=1$ and $T=0.1$ when $\phi_d=2\pi$ & $\phi_s=2\pi$.

Figure 4(a-e) depicts the variation of FWHM with the apodization parameter β in the presence of defocus and primary spherical aberration with transmission factor T is 0.1 and partition parameter for the central zone ε is 0.1 with phase. The apodization parameter β is increased from 0 to 1 for the $\beta=0$ and 0.6 the optical side lobes

are completely suppressed, for higher orders of apodization parameter $\beta=1$ the radius of the first dark ring should be less than that of airy case.

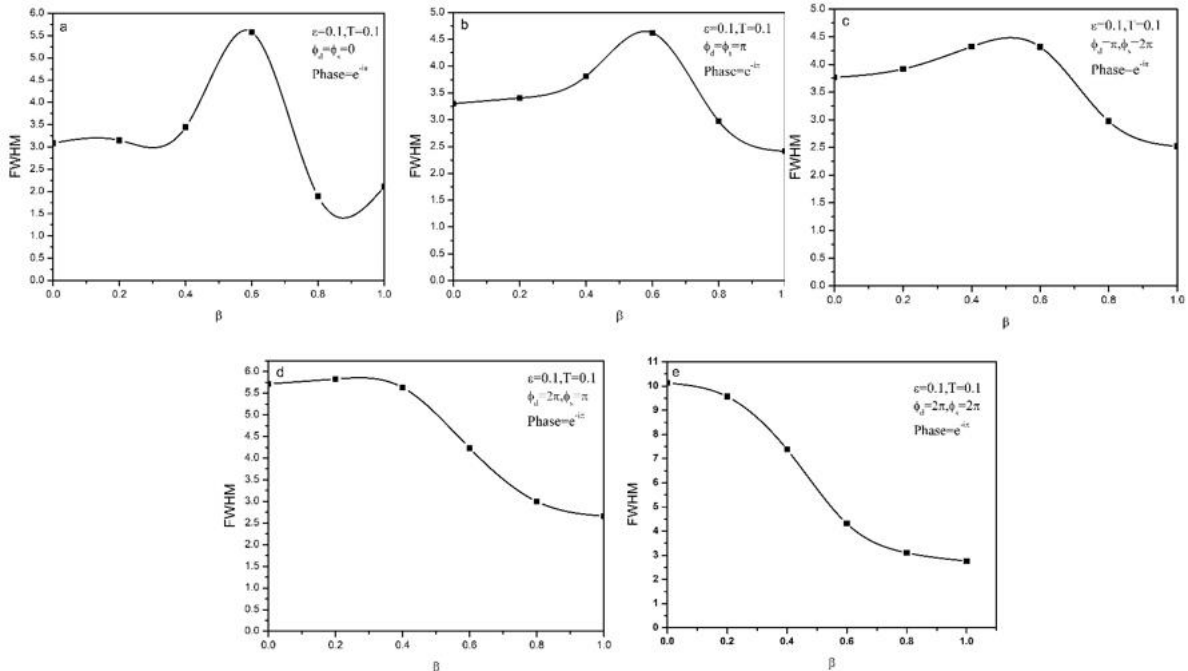


Fig.4 Variation of FWHM with β for (a) $\phi_d=0$ & $\phi_s=0$, (b) $\phi_d=\pi$ & $\phi_s=\pi$, (c) $\phi_d=\pi$ & $\phi_s=2\pi$, (d) $\phi_d=2\pi$ & $\phi_s=\pi$, (e) $\phi_d=2\pi$ & $\phi_s=2\pi$ for value of T with Phase of π

It is also observed that, FWHM decreased for higher values of β with induced phase π and it attains minimum for $\beta=1$ and $T=0.1$ when $\phi_d=2\pi$ & $\phi_s=2\pi$. It is more clearly shown from the Table2.

Phase= $e^{-i\pi}$, $\epsilon=0.1$, $T=0.1$

FWHM					
β	$\phi_d=\phi_s=0$	$\phi_d=\phi_s=\pi$	$\phi_d=\pi, \phi_s=2\pi$	$\phi_d=2\pi, \phi_s=\pi$	$\phi_d=2\pi, \phi_s=2\pi$
0	3.0855	3.3023	3.7662	5.7148	10.1305
0.2	3.1486	3.4056	3.9188	5.8298	9.5671
0.4	3.4439	3.8134	4.3225	5.6313	7.3782
0.6	5.5787	4.6209	4.3178	4.2302	4.3146
0.8	1.8939	2.9704	2.9753	2.9982	3.1051
1	2.1078	2.4141	2.5195	2.66	2.7651

Table 2: Full Width Half Maxima values

III. Conclusions

In this work, the intensity distribution of the PSF is determined for different values of β under the combined effects of defocus and primary spherical aberrations. For unapodized pupil, the sidelobe region was increased dynamically with increasing the values of ϕ_d and ϕ_s . By employing the amplitude apodizer along with the phase across the exit pupil, the sidelobes and the presence of non-zero first minima are greatly eliminated. It is clear that the apodization pupil at ($\beta = 0.6$) gradually improved the performance of aberrated optical systems at higher degrees of defocus and primary spherical aberration specially, when transmission factor $T=0.1$ and for apodization parameter $\beta = 1$ it reached maximum intensity with suppressed side lobes hence forma a super resolver. Suppressing optical side lobes on either side of the diffracted point source explicitly allows us to detect the position of a faded point source in all directions around the apodized one. Finally, the Hanning apodization pupil with the induced phase is optimal in decreasing the FWHM and hence the coherent optical system is able to resolve the two overlapping point sources.

References

- [1]. Hecht, E., Zajac, A., "Optics", (Addison – Wesley, USA), 2nd Ed., p.422, 496, 497 & 512, (1987).
- [2]. Wetherell, W.B. "Applied optics and optical engineering" (Academic press, N.Y., Eds. R. R. Shannon & J.C. Wyant) vol.8, ch.6, p.173-283, (1980).
- [3]. Papoulis, A., "Maximum Intensity of Diffraction Patterns and Apodization", J. Opt. Soc. Am., 57, p.362,(1967). DOI:10.1364/JOSA.57.000362
- [4]. Papoulis, A., "Systems and Transforms with Applications in Optics", (McGraw-Hill, USA) p.442, (1968).
- [5]. K. P. Rao, P. K. Mondal, and T. Seshagiri Rao, "Coherent imagery of straight edges with Straubelapodisation filters," *Optik*, 50, p 73–81 (1978).
- [6]. BARAKAT, R., "SOLUTION OF THE LUNEBERG APODIZATION PROBLEMS", J. OPT. SOC. AM., 52, P.264, 276 & 985, (1962).doi:10.1364/JOSA.52.000264
- [7]. J. P. Mills and B. J. Thompson, Effect of aberrations and apodization on the performance of coherent optical systems. II. *Imaging*, Vol 3, pp 704, (1986).
- [8]. Venkanna M. and Karuna Sagar D., "Reduction in edge-ringing in aberrated images of coherent edge objects by multishaded aperture", J. of Advances in optics (2014). DOI:10.1155/2014/963980
- [9]. P.K Katti and B.N. Gupta, Effect of Amplitude filter on the partially Space Coherent diffraction of a Defocused optical System, J. Opt. Soc. Am. 62, 1, 41-44 (1972)
- [10]. Hubert F. A Tschunko, Apodization and Image Contrast, *Appl.Opt.* 18, 7, 955 (1979)
- [11]. T.Araki and T. Asakura, Coherent Apodization Problems, *Opt.Commu.*20, 3,373-377 (1997)
- [12]. Venkanna M. and Karuna Sagar D., "Amplitude filters in shaping the point spread function of optical imaging systems", Proc. of SPIE, 9654, p.A1, (2015). DOI: 10.1117/12.2181610
- [13]. Venkanna M, Sagar KD., Edge imaging characteristics of aberrated coherent optical systems by edge masking of circular apertures, *Computer Optics*, 46(3): 388-394(2022). DOI: 10.18287/2412-6179-CO-940.
- [14]. Leaver FG, Smith RW, 1973, Use of Apodization in Coherent Imaging Systems, *Optik*, 39:156-160
- [15]. Considine. P.S., "Effects of Coherence on Imaging Systems", J. Opt. Soc. Am., 56, p.1001, (1966). DOI:10.1364/JOSA.56.001001
- [16]. Jacquinot P, Roizen-Dossier B. II Apodization. *Prog.in Optics* 1964; 3: 29-186. DOI:10.1016/S0079-6638(08)70570-5
- [17]. Siu GG, Cheng L, Chiu DS. Improved side-lobe suppression in asymmetric apodization. *J Phys D: Appl Phys* 1994; 27(3): 459-463. DOI: 10.1088/0022-3727/27/3/005
- [18]. Dowski ER, Cathey WT. Extended depth of field through wavefront coding. *ApplOpt* 1995; 34(11): 1859-1866. DOI: 10.1364/AO.34.001859.
- [19]. Pan C, Chen J, Zhang R, Zhuang S. The extension ratio of depth of field by wavefront coding method. *Opt Ex-press* 2008; 16(17): 13364-13371. DOI: 10.1364/OE.16.013364.
- [20]. Khonina SN, Ustinov AV. Generalized apodization of an incoherent imaging system aimed for extending the depth of focus. *Pattern Recognition and Image Analysis* 2015; 25(4): 626-631. DOI: 10.1134/S1054661815040100
- [21]. Dzyuba A.P., Serafimovich P.G., Khonina S.N., Popov S.B., Application of a neural network for calculating the surface relief of a different level two-zone lens with an increased depth of field, Proc. of SPIE Vol. 11516, 115161A (2020); DOI:10.1117/12.2565993.
- [22]. Khonina S.N., Volotovskiy S.G., Dzyuba A.P., Serafimovich P.G., Popov S.B., and Butt M.A., Power phase apodization study on compensation defocusing and chromatic aberration in the imaging system, *Electronics (MDPI)* 10, 1327-(15p), (2021); DOI:10.3390/electronics10111327
- [23]. Barakat R. Application of apodization to increase Two-point resolution by Sparrow criterion under incoherent illumination. *JOSA* 1962; 52(3): 276-283. DOI: 10.1364/JOSA.52.000276.
- [24]. Kowalczyk M, Zapata-Rodriguez CJ, Martinez-Corral M. Asymmetric apodization in confocal scanning systems. *ApplOpt* 1998; 37(35): 8206-8214
- [25]. Khonina S.N. and Ustinov A.V., Sharper focal spot for a radially polarized beam using ring aperture with phase jump, *Journal of Engineering (Hindawi Publishing Corporation)*, ID 512971, 8 pp. (2013) DOI: 10.1155/2013/512971
- [26]. Reddy A. N. K., Sagar D. K., Khonina S. N., Complex pupil masks for aberrated imaging of closely spaced objects, *Optics and Spectroscopy*, 123(6) 940–949 (2017), DOI: 10.1134/S0030400X17120189
- [27]. Reddy, A.N.K., Khonina S.N., Apodization for improving the two-point resolution of coherent optical systems with defect of focus, *Applied Physics B* 124, 229-(9p) (2018); DOI: 10.1007/s00340-018-7101-z
- [28]. Reddy A.N.K., Hashemi M., Khonina S.N., Apodization of two-dimensional pupils with aberrations, *Pramana – Journal of Physics* 90, 77-(8p) (2018); DOI: 10.1007/s12043-018-1566-5
- [29]. Hopkins HH, Zalar B. Aberration tolerances based on line spread function. *J Mod Opt* 1987; 34(3): 371-406. DOI: 10.1080/09500348714550391
- [30]. Sheppard CJR, Choudhury A. Annular pupils, radial polarization, and superresolution. *ApplOpt* 2004; 43(22): 4322-4327. DOI: 10.1364/AO.43.004322
- [31]. Ratnam C, Lakshman Rao V, Goud SL. Comparison of PSF maxima and minima of multiple annuli coded aperture (MACA) and complementary multiple annuli coded aperture (CMACA) systems. *J Phys D: Appl Phys* 2006; 39: 4148-4152. DOI: 10.1088/0022-3727/39/19/005.
- [32]. Khonina SN, Ustinov AV, Pelevina EA. Analysis of wave aberration influence on reducing the focal spot size in a high-aperture focusing system. *J Opt* 2011; 13(9): DOI: 10.1088/2040-8978/13/9/095702
- [33]. Khonina S.N., Volotovskiy S.G., Minimizing the bright/shadow focal spot size with controlled side-lobe in-crease in high-numerical-aperture focusing systems, *Advances in Optical Technologies (Hindawi Publishing Corporation)*, Volume 2013, Article ID 267684, 13pages, DOI: 10.1155/2013/267684.

N. Sabitha, et. al. "Point Spread Functions of defocused Leaky Annular Apertures with Spherical Aberration." *IOSR Journal of Applied Physics (IOSR-JAP)*, 15(2), 2023, pp. 43-49.